

Joint Direction and Frequency Estimation with Small Array Receiver

Shu Wang
LG Electronics Mobile Research
San Diego, CA 92131-1639

James Caffery, Jr.
University of Cincinnati
Cincinnati, OH 45221-0030

Hanhong Shen
Qualcomm Incorporated
San Diego, CA 92121-1714

Abstract—Several high-resolution subspace schemes for jointly estimating the direction and frequency of each arriving signal with a small ESPRIT array receiver are presented, in which the physical size of array can be much smaller than the number of simultaneously tracked signals. With signal spectral analysis, a special signal parameter matrix is constructed so that the direction and frequency of each signal are estimated directly from its eigenvalue and eigenvector pair. No searching or pairing procedure is necessary. With further analysis of the correlation matrix properties, some enhancements with space-time preprocessing and total least squared estimation are given. Besides that the Cramér-Rao lower bound is given for performance discussion, the first-order approximation of the asymptotic mean squared estimation errors is also derived and discussed. Computer simulations are presented to demonstrate the performance of the proposed schemes.

I. INTRODUCTION

The application of antenna array is expected to help reduce co-channel interference, extend coverage, increase spectral efficiency and therefore fulfill increasing demand for higher capacity and more services from the existing or next-generation wireless communication systems [1], [2]. With array signal processing, both transmitter and receiver can benefit from better channel estimation, more accurate signal steering and less interference [1]. With multiple-antenna transmission, higher spectrum efficiency is achievable without increasing transmit power [2]. In these applications, high-resolution signal parameter estimation, e.g., direction or frequency-of-arrival (DOA/FOA) estimation, within the output data of an array of antennas at different locations in space and/or time domain of a wave-field is frequently studied [1]. Roy et al. proposed a patented subspace rotation approach, ESPRIT, for signal parameter estimation, which can be used for finding the direction or frequency in a computationally efficient manner [3]. It is search-free and fairly robust with no array calibration information and its performance is close to the calibrated Cramér-Rao lower bound (CRLB) for many cases of practical interest [3]. All these make it very competitive with many other algorithms [1].

Though the generalization of so-called high-resolution one dimensional (1D) algorithms to two-dimensional (2D) cases is relatively straightforward, the main difficulty associated with these methods is that both computation and storage costs tend to increase rapidly with the number of dimensions of the parameter vector due to searching [4], [5] and possible non-

trivial pairing procedures [6], [7]. Since those high-resolution 2D methods have a considerably higher computational cost, many implementations employ non-parametric techniques in practice, e.g., Butler beam scanning. These non-parametric techniques are less complicated but their performance is known to be poor [8]. Additionally, most modern high-resolution techniques require that the antenna array size must be greater than the number of signal sources to avoid ambiguity problem. This, in turn, may further render the applicability of these techniques unattractive [9]. And this also make it a very important topic to design the receivers tracking many more signal sources than the employed array size and also understand the tradeoffs between array size and estimation accuracy.

In this paper, several joint direction and frequency estimation algorithms using small ESPRIT array are presented and discussed, where the antenna array consists of several doublets the number of which is less than the number of tracked signals. Different to conventional ESPRIT and other 2D high-resolution estimation approaches, a special signal parameter matrix is constructed with each eigenvalue/eigenvector pair associated the direction/frequency of a tracked signal. This makes the proposed algorithms computation efficient with no search or pairing procedure necessary and attractive for practical implementation. Besides this, with additional analysis of the estimation of involved correlation matrices, two enhancements are outlined too. One enhancement is to perform a space-time preprocessing on correlation matrix and the other one is to improve the signal parameter estimation accuracy with total least squared (TLS) estimation instead of the regular least squared (LS) estimation. In addition to the formulation of the 2D CRLB on our approaches, an asymptotic analysis of the estimation performance with first-order approximation is given. Compared with the 2D CRLB, this asymptotic analysis is more algorithm-specific and accurate. It also gives more insights of the proposed algorithms. Computer simulations are also presented to support our conclusions.

II. SYSTEM MODEL AND PROBLEM DESCRIPTION

Let's assume there are K uncorrelated narrow-band radiating sources which emit plane wave signals, $s_k(t)$, with different center frequencies, f_k , from distinct directions, θ_k , $k = 1, 2, \dots, K$, corrupted by a additive Gaussian white noise (AWGN) with variance, σ^2 , at the array receiver. This is a

typical scenario happened in most wireless communication, especially in the reverselink. We assume that the plane waves and additive noise are stationary zero-mean processes and uncorrelated from sensor to sensor. The complex form of the observed signal $r_m(t)$ at the m th antenna element of the array can be expressed as

$$r_m(t) = \sum_{k=1}^K a_m(f_k, \theta_k) s_k(t) e^{-j2\pi f_k t} + n_m(t) \quad (1)$$

where $a_m(f_k, \theta_k)$ denotes the complex response, including both the gain $g_{m,k} = |a_m(f_k, \theta_k)|$ and the phase $\phi_{m,k} = \arg\{a_m(f_k, \theta_k)\}$, of antenna m at frequency f_k and direction θ_k , $s_k(t)$ is the narrow-band signal and the length of array receiver is M . The observed array signal samples can also be expressed in time-domain vector and matrix form as

$$\begin{aligned} \mathbf{r}_T^{(m)}(t) &= [r_m(t) \cdots r_m(t + (L-1)T_s)]^T \\ &= \mathbf{A}_T^* \mathbf{s}(t) + \mathbf{n}_T^{(m)}(t) \end{aligned} \quad (2)$$

and

$$\begin{aligned} \mathbf{R}(t) &= [\mathbf{r}_T^{(1)}(t) \mathbf{r}_T^{(2)}(t) \cdots \mathbf{r}_T^{(M)}(t)]^T \\ &= \mathbf{A}_S \mathbf{S}(t) \mathbf{A}_T^H + \mathbf{N}(t) \end{aligned} \quad (3)$$

where $\mathbf{r}_T^{(m)}(t)$ is a $L \times 1$ vector of L consecutive samples at the m th antenna. $\mathbf{R}(t)$ is the $M \times L$ signal matrix constructed with the temporal signal vectors $\{\mathbf{r}_T^{(m)}(t) : t = 0, 1, \dots, L-1\}$. The parameter $T_s = \frac{1}{f_s}$ denotes the sample period which is the inverse of the sampling frequency, f_s , $[\cdot]^*$ denotes the complex conjugate operator, $[\cdot]^T$ denotes the transpose operator and $[\cdot]^H$ denotes the complex conjugate transpose operator. In (3), \mathbf{A}_S is labelled as $M \times K$ *spatial steering matrix* written by

$$\mathbf{A}_S = [\mathbf{a}_S(f_1, \theta_1) \mathbf{a}_S(f_2, \theta_2) \cdots \mathbf{a}_S(f_K, \theta_K)] \quad (4)$$

of which the k th column $\mathbf{a}_S(f_k, \theta_k)$ denotes the $M \times 1$ *spatial steering vector*, defined by

$$\mathbf{a}_S(f_k, \theta_k) = [a_1(f_k, \theta_k) \cdots a_M(f_k, \theta_k)]^T \quad (5)$$

for the k th arriving wave-front $s_k(t)$. Likewise, \mathbf{A}_T is labelled as $L \times K$ *temporal steering matrix* expressed by

$$\mathbf{A}_T = [\mathbf{a}_T(f_1) \mathbf{a}_T(f_2) \cdots \mathbf{a}_T(f_K)] \quad (6)$$

of which the k th column

$$\mathbf{a}_T(f_k) = \begin{bmatrix} 1 & e^{j2\pi \frac{f_k}{f_s}} & e^{j4\pi \frac{f_k}{f_s}} & \cdots & e^{j2\pi(L-1) \frac{f_k}{f_s}} \end{bmatrix}^T \quad (7)$$

is a $L \times 1$ *temporal steering vector*. In (2) and (3), $\mathbf{s}(t)$ and $\mathbf{S}(t)$ are the $K \times 1$ signal vector and $K \times K$ signal diagonal matrix, respectively defined by

$$\mathbf{s}(t) = [s_1(t) \ s_2(t) \ \cdots \ s_K(t)]^T \quad (8)$$

and

$$\mathbf{S}(t) = \text{diag}\{[s_1(t) \ s_2(t) \ \cdots \ s_K(t)]\} \quad (9)$$

for the K carrier signals. $\mathbf{n}_T^{(m)}(t)$ and $\mathbf{N}(t)$ are the corresponding $L \times 1$ noise vector and $M \times L$ noise matrix, respectively.

The DOA/FOA estimation problem is to estimate the direction-frequency pairs $\{(f_k, \theta_k) : k = 1, 2, \dots, K\}$, providing (2) and (3) are available. This can be done with some linear signal processing approaches, such as Butler beam scanning or 2D Fourier spectrum analysis on received signals $\{r_m(t) : 1 \leq m \leq M\}$. However, the resolution of these linear approaches typically may not be good high enough for many applications. Here we propose several high-resolution signal parameter estimation approaches with signal spectrum analysis and a small ESPRIT array. Compared with other popular array structures like uniform linear array (ULA) and uniform circular array (UCA), ESPRIT array consisting of multiple doublets has flexible structure and doesn't require calibration between doublets. This makes it very attractive for practical deployment. Besides this, most wireless system is required to serve more users with a small-size array in reality. This becomes more critical when the system operates in a large number of frequency bands. This is because of not only the large number of users being simultaneously served but also the size limitation of most receivers. Therefore, it is very important to estimate signal parameters using small array and understand the tradeoff between array size and estimation accuracy.

III. JOINT DOA/FOA ESTIMATION WITH ESPRIT ARRAY

We assume a simple uncalibrated ESPRIT array consisting of two subarrays \mathcal{X} and \mathcal{Y} of the same length M . They are identical and separated by a fixed distance d . Each pair of identical elements of these two subarrays may be called *doublet*. The directional gain and phase response of these doublets may be completely different. This requirement makes the necessary array calibrate much easier in reality. The relationship between the carrier signals received by subarray \mathcal{X} and \mathcal{Y} is

$$\mathbf{S}^x(t) = \mathbf{S}^y(t) \mathbf{D}_S \quad (10)$$

where $\mathbf{S}^x(t)$ and $\mathbf{S}^y(t)$ denote the signal matrix $\mathbf{S}(t)$ received by subarray \mathcal{X} and \mathcal{Y} at time t , respectively, and

$$\mathbf{D}_S = \text{diag}\left\{ \left[e^{j2\pi f_1 \frac{d \sin \theta_1}{c}} \cdots e^{j2\pi f_K \frac{d \sin \theta_K}{c}} \right] \right\} \quad (11)$$

denotes the spatial rotation diagonal matrix, which includes the information of the direction-frequency pairs $\{(f_k, \theta_k) : k = 1, 2, \dots, K\}$. In order to obtain the high-resolution estimation of the direction-frequency pairs, it is necessary to analysis the signal spectral structure of (3). For this, the time-domain correlation matrices of the outputs of subarray \mathcal{X} and \mathcal{Y} can be expressed by

$$\mathbf{R}_T^{xx} = \frac{1}{M} \mathbf{E}\{\mathbf{X}^H(t) \mathbf{X}(t)\} = \mathbf{A}_T \mathbf{P}_s \mathbf{A}_T^H + \sigma^2 \mathbf{I} \quad (12)$$

and

$$\mathbf{R}_T^{yx} = \frac{1}{M} \mathbf{E}\{\mathbf{Y}^H(t) \mathbf{X}(t)\} = \mathbf{A}_T \mathbf{P}_s \mathbf{D}_S \mathbf{A}_T^H \quad (13)$$

where \mathbf{X} and \mathbf{Y} denote the signal matrix \mathbf{R} received by subarray \mathcal{X} and \mathcal{Y} , respectively.

With (12) and (13), a special signal parameter matrix \mathbf{R} is defined by

$$\mathbf{R} = \bar{\mathbf{R}}_T^{xx} + \mathbf{R}_T^{yx} = (\mathbf{R}_T^{xx} - \sigma^2 \mathbf{I})^+ \mathbf{R}_T^{yx} \quad (14)$$

with $\bar{\mathbf{R}}_T^{xx} = \mathbf{R}_T^{xx} - \sigma^2 \mathbf{I}$ denoting the correlation matrix of subarray \mathcal{X} or \mathcal{Y} with no noise. Furthermore, when the ranks of \mathbf{A}_T and \mathbf{P}_s are K , the k th column of the temporal steering matrix \mathbf{A}_T is the eigenvector of the signal parameter matrix \mathbf{R} , which in turn corresponds to the k th diagonal element of the diagonal matrix \mathbf{D}_S . This can be expressed by

$$\mathbf{R}\mathbf{A}_T = \mathbf{A}_T\mathbf{D}_S. \quad (15)$$

With (15), the frequency and direction of each signal source can be estimated from one pair of an eigenvector and a nonzero eigenvalue. As a result, they are automatically coupled. No additional search or pairing procedure is necessary. No knowledge of the subarray responses is required, either. Furthermore, we can see that, in (14), the size of the square matrix \mathbf{R} is M , which can be set to an arbitrary number regardless of the physical array length. This means that even with a single doublet, it is still possible to estimate as many incoming signals as desired, provided that there are enough array measurements available. Finally, the question left is how to estimate the signal parameter matrix \mathbf{R} with the estimates $\hat{\mathbf{R}}_T^{xx}$ and $\hat{\mathbf{R}}_T^{yx}$ of the correlation matrices defined in (12) and (13) available. Here two estimation schemes, LS estimation and TLS estimation, and one pre-processing enhancement are presented.

A. Least Squares Estimation

The least square estimation of \mathbf{R} is the solution to the following optimization problem and can be expressed by

$$\mathbf{R}_{LS} = \min_{\mathbf{Z}} \left\| \hat{\mathbf{R}}_T^{yx} - \tilde{\mathbf{R}}_T^{xx} \mathbf{Z} \right\|_2 = \tilde{\mathbf{R}}_T^{xx} + \hat{\mathbf{R}}_T^{yx} \quad (16)$$

where $\hat{\mathbf{R}}_T^{yx}$ and $\tilde{\mathbf{R}}_T^{xx}$ denote the estimate of \mathbf{R}_T^{yx} and $\bar{\mathbf{R}}_T^{xx}$, respectively.

B. Total Least Squares Estimation

In (16), it is assumed that $\tilde{\mathbf{R}}_T^{xx}$ is equal to $\bar{\mathbf{R}}_T^{xx}$. This is not always true, though they may be very close. Given noisy measurements, both the estimated matrix $\hat{\mathbf{R}}_T^{xx}$ and $\hat{\mathbf{R}}_T^{yx}$ contain errors. Hence, the LS estimate will inherently be biased [10]. It seems reasonable to treat the uncertainties in the matrices symmetrically. In order to utilize both information from $\hat{\mathbf{R}}_T^{xx}$ and $\hat{\mathbf{R}}_T^{yx}$, the following optimization problem is presented to estimate the signal parameter matrix \mathbf{R} :

$$\mathbf{R}_{TLS} = \min_{\mathbf{Z}} \left\| \begin{bmatrix} \tilde{\mathbf{R}}_T^{xx} \\ \hat{\mathbf{R}}_T^{yx} \end{bmatrix} - \begin{bmatrix} \bar{\mathbf{R}}_T^{xx} \\ \hat{\mathbf{R}}_T^{yx} \mathbf{Z} \end{bmatrix} \right\|_2. \quad (17)$$

Solving the minimization problem in (17) results in a total least squares estimate of the \mathbf{R} [10], which maps the columns of $\tilde{\mathbf{R}}_T^{xx}$ onto those of $\hat{\mathbf{R}}_T^{yx}$. The TLS estimate of the signal parameter matrix, \mathbf{R}_{TLS} , can be presented as

$$\mathbf{R}_{TLS} = (\tilde{\mathbf{R}}_T^{xxT} \tilde{\mathbf{R}}_T^{xx} - \sigma_{K+1}^2 \mathbf{I}) + \tilde{\mathbf{R}}_T^{xxT} \hat{\mathbf{R}}_T^{yx} \quad (18)$$

where σ_{K+1} is the $(K+1)$ st largest eigenvalue of $[\tilde{\mathbf{R}}_T^{xxT} \hat{\mathbf{R}}_T^{yx}]$.

C. Space-Time Processing Improvement

It is knowingly very important to obtain accurate estimates of the correlation matrices in the subspace algorithms. The correlation matrices defined in (12) and (13) can be directly estimated with time-domain averaging expressed by

$$\begin{aligned} \hat{\mathbf{R}}_T^{xx} &= \frac{1}{MN} \sum_{n=1}^N \mathbf{X}(t - nT_s) \mathbf{X}^H(t - nT_s) \\ \hat{\mathbf{R}}_T^{yx} &= \frac{1}{MN} \sum_{n=1}^N \mathbf{X}(t - nT_s) \mathbf{Y}^H(t - nT_s). \end{aligned} \quad (19)$$

Obviously, the estimates in (19) only utilize the property of the received signal that it is stationary in the time-domain, though the received signal $r_m(t)$ is also assumed to be stationary in the space-domain. Hence, when $r_i(t)$ is stationary both in space and time, the matrices \mathbf{R}_T^{xx} and \mathbf{R}_T^{yx} are Toeplitz matrices and can be estimated by

$$\mathbf{R}_T^{xx} = \mathbf{R}_T^{xxH} = \begin{bmatrix} r_0^{xx} & r_1^{xx*} & \cdots & r_{L-1}^{xx*} \\ r_1^{xx} & r_0^{xx} & \cdots & r_{L-2}^{xx*} \\ \vdots & \vdots & \ddots & \vdots \\ r_{L-1}^{xx} & r_{L-2}^{xx} & \cdots & r_0^{xx} \end{bmatrix} \quad (20)$$

where

$$r_p^{xx} = \frac{1}{2M(L-p)} \sum_{m=1}^M \sum_{l=1}^{L-p} \mathbb{E} \{ r_m^x(t - lT_s) r_m^{x*}(t - (l+p)T_s) + r_m^y(t - lT_s) r_m^{y*}(t - (l+p)T_s) \} \quad (21)$$

$p = 0, 1, \dots, L-1$, and

$$\mathbf{R}_T^{yx} = \begin{bmatrix} r_0^{yx} & r_{-1}^{yx} & \cdots & r_{-L+1}^{yx} \\ r_1^{yx} & r_0^{yx} & \cdots & r_{-L+2}^{yx} \\ \vdots & \vdots & \ddots & \vdots \\ r_{L-1}^{yx} & r_{L-2}^{yx} & \cdots & r_0^{yx} \end{bmatrix} \quad (22)$$

where

$$\begin{aligned} r_q^{yx} &= \frac{1}{M(L-q)} \sum_{m=1}^M \sum_{l=1}^{L-q} \mathbb{E} \{ r_m^{y*}(t - (l+q)T_s) r_m^x(t - lT_s) \} \\ r_{-q}^{yx} &= \frac{1}{M(L-q)} \sum_{m=1}^M \sum_{l=1}^{L-q} \mathbb{E} \{ r_m^{y*}(t - lT_s) r_m^x(t - (l+q)T_s) \} \end{aligned} \quad (23)$$

$q = 0, 1, \dots, L-1$. These space-time joint averaging on the collected data should improve the estimate of the correlation matrices which should be much closer to the theoretical values. Thus, it is expected that the performance of the proposed joint DOA/FOA estimation algorithm is improved as well.

IV. PERFORMANCE ANALYSIS

A. Analysis of Estimation Errors

It is not easy to give a close-form expression for the proposed DOA/FOA estimation schemes which extend the classic ESPRIT algorithm since the directions and frequencies are directly associated with the eigenvalues and eigenvectors of the matrix \mathbf{R} . But we know that in both the LS and TLS

estimates of the matrix \mathbf{R} , the following expression holds regarding the errors in the matrices $\bar{\mathbf{R}}_T^{xx}$, \mathbf{R}_T^{yx} and \mathbf{R} [11]:

$$\Delta \mathbf{R} \approx \bar{\mathbf{R}}_T^{xx+} (\Delta \mathbf{R}_T^{yx} - \Delta \bar{\mathbf{R}}_T^{xx} \mathbf{R}) . \quad (24)$$

When $\|\Delta \mathbf{R}\|$ is very small, we can give the following first-order approximation of the errors in f_i , θ_i , $i = 1, 2, \dots, K$.

$$\Delta f_i \approx -j \frac{3f_s}{\pi(L-1)L(2L-1)} \mathbf{a}_i^H \mathbf{W} (\mathbf{R} - \lambda_i \mathbf{I})^+ (\Delta \lambda_i \mathbf{I} - \Delta \mathbf{R}) \mathbf{a}_i \quad (25)$$

and

$$\begin{aligned} \Delta \theta_i \approx & -j \frac{c}{2\pi f_i d \cos \theta_i} \mathbf{v}_i^H \bar{\mathbf{R}}_T^{xx+} (\Delta \mathbf{R}_T^{yx} - \lambda_i \Delta \bar{\mathbf{R}}_T^{xx}) \mathbf{u}_i \\ & + j \frac{3f_s \tan \theta_i}{\pi(L-1)L(2L-1)f_i} \mathbf{a}_i^H \mathbf{W} (\mathbf{R} - \lambda_i \mathbf{I})^+ (\Delta \lambda_i \mathbf{I} - \Delta \mathbf{R}) \mathbf{a}_i, \end{aligned} \quad (26)$$

where λ_i , \mathbf{v}_i and \mathbf{u}_i denote the i th eigenvalue, and the left- and right-eigenvector of \mathbf{R} , respectively, \mathbf{a}_i denotes the steering vector $\mathbf{a}_T(f_i)$, $\mathbf{W} = \text{diag}\{0, 1, \dots, (L-1)\}$, j denotes the imaginary unit and $\Delta \cdot$ denotes the error in a scalar, vector or matrix.

B. Cramér-Rao Lower Bound

The CRLB is given by the inverse of the Fisher information matrix (FIM). To compute the FIM, we first define the parameter vector $\phi = [\sigma^2, \mathbf{s}_R^T, \mathbf{s}_I^T, \boldsymbol{\theta}^T, \mathbf{f}^T]^T$, where $\mathbf{s}_R(t) = \Re\{\mathbf{s}(t)\}$, $\mathbf{s}_I(t) = \Im\{\mathbf{s}(t)\}$, $\boldsymbol{\theta} = [\theta_1, \dots, \theta_K]^T$, and $\mathbf{f} = [f_1, \dots, f_K]^T$. Then, the FIM is defined to be

$$\text{FIM} = \text{CRLB}^{-1} = \mathbb{E} \left\{ \left(\frac{\partial \ln L}{\partial \phi} \right) \left(\frac{\partial \ln L}{\partial \phi} \right)^H \right\} \quad (27)$$

where, with the data model in (2) and (3), $\ln L$ is the log-likelihood function given by

$$\ln L = C - LMK \ln \sigma^2 - \frac{1}{2\sigma^2} \sum_{t=1}^N \sum_{l=0}^{L-1} \|\mathbf{e}(t - lT_s)\|_2^2 \quad (28)$$

with C being a constant and $\mathbf{e}(t - lT_s) = \mathbf{r}(t - lT_s) - \mathbf{A}_S \mathbf{D}_T^l \mathbf{s}(t)$.

It can be shown that the CRLB for the parameters of interest ($\boldsymbol{\theta}$ and \mathbf{f}) are

$$\begin{aligned} \text{CRLB}(\boldsymbol{\theta}) &= \mathcal{P}^{-1} + \mathcal{P}^{-1} \mathcal{Q}^T [\mathcal{Q} - \mathcal{O} \mathcal{P}^{-1} \mathcal{O}^T]^{-1} \mathcal{O} \mathcal{P}^{-1} \\ \text{CRLB}(\mathbf{f}) &= [\mathcal{Q} - \mathcal{O} \mathcal{P}^{-1} \mathcal{O}^T]^{-1} \end{aligned} \quad (29)$$

where

$$\begin{aligned} \mathcal{O} &= \boldsymbol{\Lambda}_{\mathbf{f}, \boldsymbol{\theta}} - \sum_{t=1}^N \Re\{\mathbf{B}_{\mathbf{f}}^H(t) \boldsymbol{\Phi} \mathbf{B}_{\boldsymbol{\theta}}(t)\} \\ \mathcal{P} &= \boldsymbol{\Lambda}_{\boldsymbol{\theta}} - \sum_{t=1}^N \Re\{\mathbf{B}_{\boldsymbol{\theta}}^H(t) \boldsymbol{\Phi} \mathbf{B}_{\boldsymbol{\theta}}(t)\} \\ \mathcal{Q} &= \boldsymbol{\Lambda}_{\mathbf{f}} - \sum_{t=1}^N \Re\{\mathbf{B}_{\mathbf{f}}^H(t) \boldsymbol{\Phi} \mathbf{B}_{\mathbf{f}}(t)\} \end{aligned} \quad (30)$$

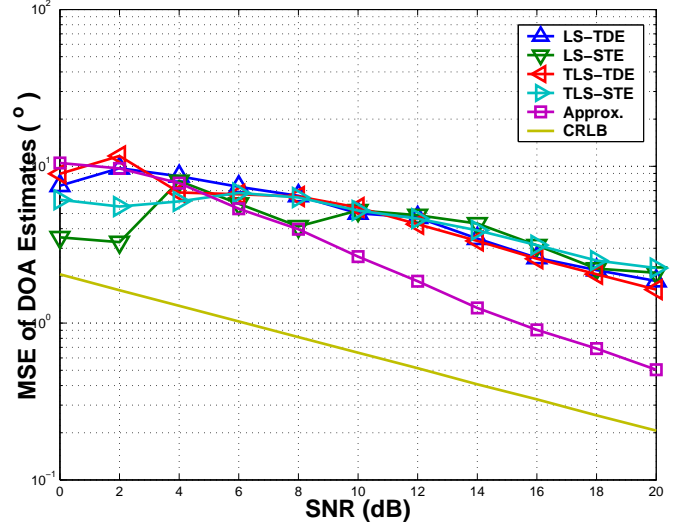


Fig. 1. MSE of DOA estimates versus SNR using one doublet, $N=500$, $L=5$, $K=4$.

and the $\boldsymbol{\Lambda}$'s, \mathbf{B} 's and $\boldsymbol{\Phi}$ are defined by

$$\begin{aligned} \boldsymbol{\Lambda}_{\mathbf{f}} &= \frac{2}{\sigma^2} \sum_{t=1}^N \sum_{l=0}^{L-1} \Re\{\mathbf{S}^H(t) \mathbf{D}_{\mathbf{f}}^{lH} \mathbf{D}_{\mathbf{f}}^l \mathbf{S}(t)\} \\ \boldsymbol{\Lambda}_{\boldsymbol{\theta}} &= \frac{2}{\sigma^2} \sum_{t=1}^N \sum_{l=0}^{L-1} \Re\{\mathbf{S}^H(t) \mathbf{D}_{\boldsymbol{\theta}}^{lH} \mathbf{D}_{\boldsymbol{\theta}}^l \mathbf{S}(t)\} \\ \boldsymbol{\Lambda}_{\mathbf{f}, \boldsymbol{\theta}} &= \frac{2}{\sigma^2} \sum_{t=1}^N \sum_{l=0}^{L-1} \Re\{\mathbf{S}^H(t) \mathbf{D}_{\mathbf{f}}^{lH} \mathbf{D}_{\boldsymbol{\theta}}^l \mathbf{S}(t)\} \end{aligned} \quad (31)$$

$$\boldsymbol{\Phi} = \frac{2}{\sigma^2} \sum_{l=0}^{L-1} \mathbf{D}_T^{lH} \mathbf{A}_S^H \mathbf{A}_S \mathbf{D}_T^l \quad (32)$$

$$\begin{aligned} \mathbf{B}_{\boldsymbol{\theta}}(t) &= \frac{2}{\sigma^2} \sum_{l=0}^{L-1} \mathbf{D}_T^{lH} \mathbf{A}_S^H \mathbf{D}_{\boldsymbol{\theta}}^l \mathbf{S}(t) \\ \mathbf{B}_{\mathbf{f}}(t) &= \frac{2}{\sigma^2} \sum_{l=0}^{L-1} \mathbf{D}_T^{lH} \mathbf{A}_S^H \mathbf{D}_{\mathbf{f}}^l \mathbf{S}(t) . \end{aligned} \quad (33)$$

V. COMPUTER SIMULATIONS

In this section, computer simulations were carried out to support the performance of the proposed algorithms. In the following simulations, the emitter signals were generated as constant amplitude planewaves with random phase, uniformly distributed on $[0, 2\pi]$. There are four incoming signals, $(+30^\circ, 5.5\text{MHz})$, $(0.0^\circ, 3.5\text{MHz})$, $(-60^\circ, 7.5\text{MHz})$ and $(+75^\circ, 1.5\text{MHz})$, simultaneously arriving at the array. The MSE of the estimates are compared with the CRLB and the approximation analysis in (25) and (26).

Case 1: Performance versus SNR

We assume there are $M = 2$ antenna elements in the array receiver, while there are $K = 4$ incoming signals. $L = 5$ and $N = 500$. The MSE of the DOA/FOA estimation of the signal source $(+30^\circ, 5.5\text{MHz})$ are calculated and shown in Figs. 1 and 2, respectively. The MSE of the estimates are

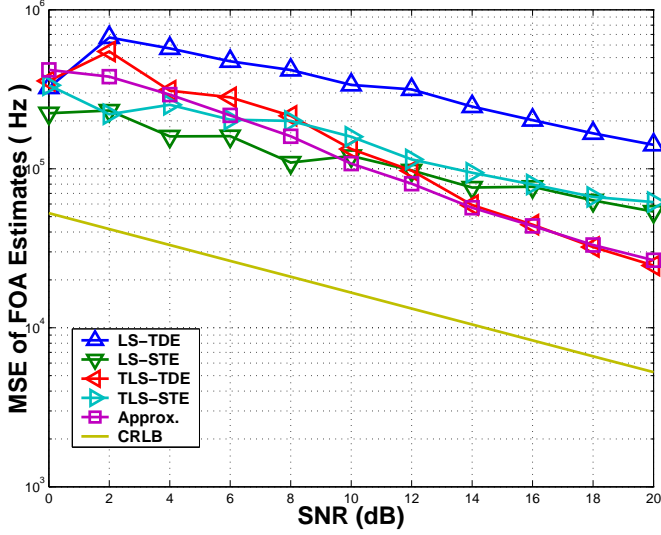


Fig. 2. MSE of FOA estimates versus SNR using one doublet, $N=500$, $L=5$, $K=4$.

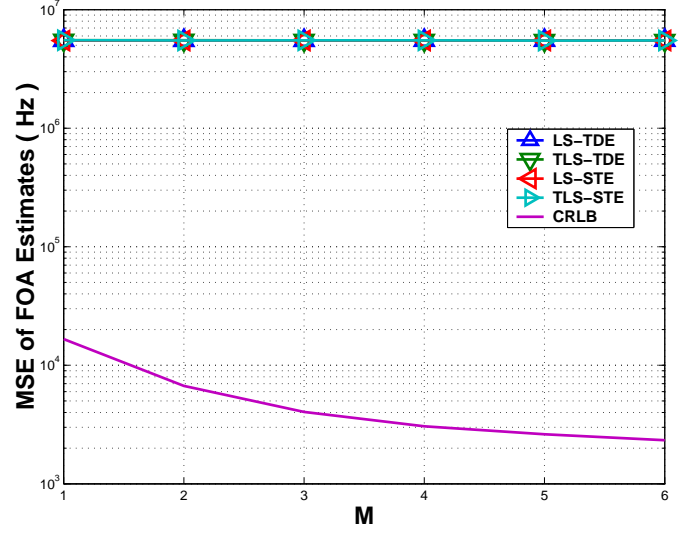


Fig. 4. MSE of FOA estimates versus M , $N = 500$, $L = 5$, $K = 4$, $\text{SNR} = 10\text{dB}$.

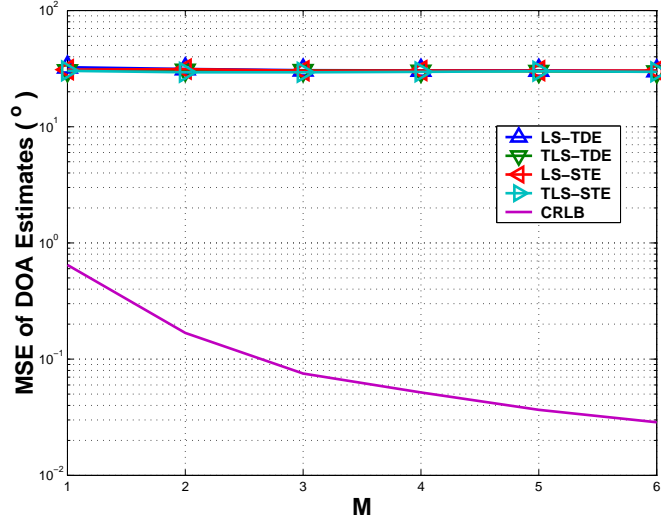


Fig. 3. MSE of DOA estimates versus M , $N = 500$, $L = 5$, $K = 4$, $\text{SNR} = 10\text{dB}$.

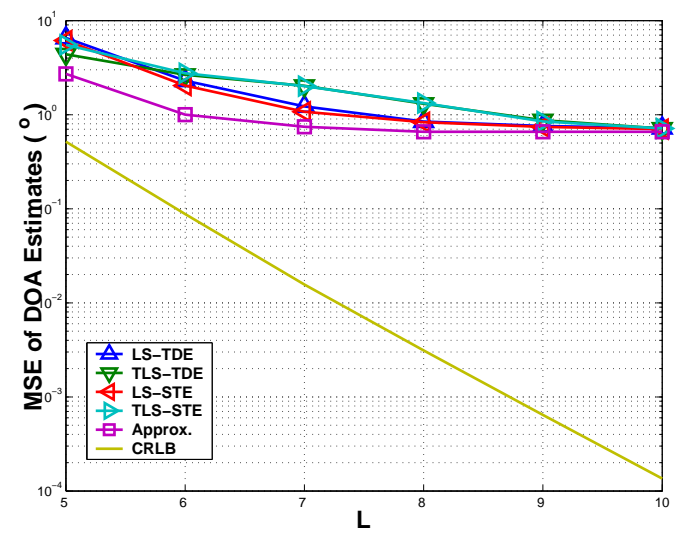


Fig. 5. MSE of DOA estimates versus L , $N=500$, $M=2$, $K=4$, $\text{SNR}=10\text{dB}$.

steadily decreasing with the increase of SNR. The performance of improved algorithms are better than LS-TDE in FOA estimation.

Case 2: Performance versus M

In Figs. 3 and 4, we examine the performance of all the proposed ESPRIT algorithms with the increase of M . There is no obvious change of the performance with the increase of M . One reason is that the increase of M is equivalent to increase the sampling number K in Eq. 12. Usually, increasing M cannot significantly improve the estimation of DOA/FOA.

Case 3: Performance versus L

In Figs. 5 and 6, we examine the performance of all the proposed ESPRIT algorithms with the increase of L . The

performance of DOA/FOA estimation becomes better. One reason is that, with the increase of L , the estimation of FOA becomes better due to more accurate subspace separation.

VI. CONCLUSIONS

In this paper, several high-resolution 2D signal parameter estimation schemes with a small ESPRIT array and signal spectral analysis are presented. They are simple and direct with no additional pairing procedure and the number of simultaneously tracked signal sources can be arbitrarily larger than array size. This makes the proposed scheme very attractive to practical implementation with less hardware cost and computation complexity.

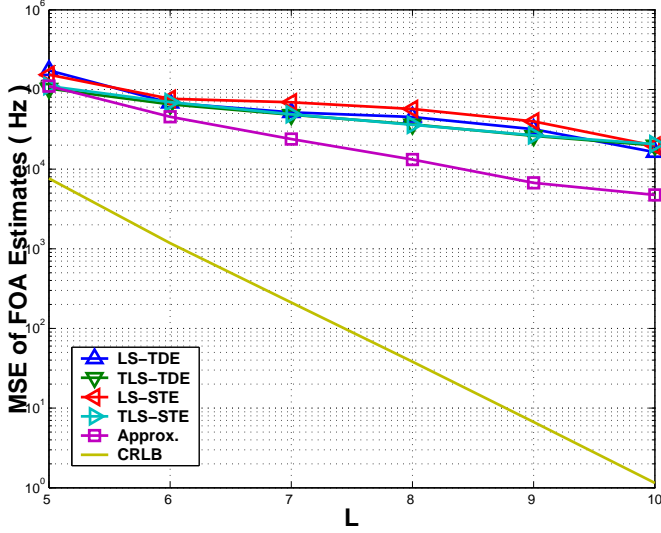


Fig. 6. MSE of FOA estimates versus L , $N = 500$, $M = 2$, $K = 4$, $\text{SNR} = 10\text{dB}$.

REFERENCES

- [1] M. Ghavami and B. (Ben) Allen. *Adaptive Array Systems: Fundamentals and Applications*. John Wiley and Sons, 2005.
- [2] M. Dohler et al. Implementable wireless access for b3g networks part i/ii/iii/iv. *IEEE Communication Magazine*, 45(3):85–111, March 2007.
- [3] R. Roy and T. Kailath. Esprit-estimation of signal parameter via rotational invariance technique. *IEEE Trans. On ASSP*, 37(7):984–995, 1989.
- [4] K. T. Wong and M. D. Zoltowski. Closed-form multi-dimensional multi-invariance esprit. In *1997 IEEE International Conference on Acoustics, Speech, and Signal Processing*, volume 5, pages 3489–3492, Munich, Germany, April 1997.
- [5] R. Bro; N. D. Sidiropoulos and G. B. Giannakis. Optimal joint azimuth-elevation and signal-array response estimation using parallel factor analysis. In *1998 Conference Record of the Thirty-Second Asilomar Conference on Signals, Systems and Computation*, volume 2, pages 1594–1598, 1998.
- [6] P. B. Ober A-J. van der Veen and E. F. Deprettere. Azimuth and elevation computation in high resolution doa estimation. *IEEE Transactions On Signal Porcessing*, 40(7):1828–1832, July 1992.
- [7] Vikas S. Kedia and Bindu Chandna. A new algorithm for 2-d doa estimation. *Signal Processing*, 60(3):325–332, August 1996.
- [8] Lal V. Godara. Application of antenna arrays to mobile communications, part ii: Beam-forming and direction-of-arrival considerations. *Proceedings of the IEEE*, 85, 1997.
- [9] Xiaodong Wang and H.V. Poor. Blind multiuser detection: A subsequence approach. *IEEE Trans. On Information Theory*, 44:677–691, March 1998.
- [10] Sabine Van Huffel and Joos Vandewalle. *The total least squares problem: computational aspects and analysis*. Society for Industrial and Applied Mathematics, 1991.
- [11] Bhaskar D. Rao and K. V. S. Hari. Performance analysis of esprit and tam in determining the direction of arrive of plane waves in noise. *IEEE Trans. On Accoustics, Speech, Signal Processing*, 37(12):1990–1995, December 1989.